50 years of QUAESTIONES GEOGRAPHICAE

OUTCROPS OF COLUMNAR ANDESITE SHAPED BY PERIGLACIAL PROCESSES – JERSAK HILLS, KING GEORGE ISLAND, ANTARCTICA

Piotr Migoń [1], Mateusz C. Strzelecki [1,2]

[1] Institute of Geography and Regional Development, University of Wrocław, Poland
[2] Alfred Jahn Cold Regions Research Centre, Institute of Geography and Regional Development, University of Wrocław, Poland

Manuscript received: January 23, 2024
Revised version: August 12, 2024

Migoń P., Strzelecki M.C., 2024. Outcrops of columnar andesite shaped by periglacial processes – Jersak Hills, King George Island, Antarctica. *Quaestiones Geographicae* 43(4), Bogucki Wydawnictwo Naukowe, Poznań pp. 5–16. 8 figs.

Abstract: This paper is an inventory of cold-climate landforms present in the andesitic Jersak Hills on King George Island in maritime Antarctica. These landforms developed under distinctive rock control imposed by columnar jointing in andesite. Multiple distinct types of slopes – ranging from low-angle rock surfaces to steep cliffs – have formed according to the spacing and inclination of joints. Numerous joints in the rock mass facilitate efficient mechanical weathering, which has produced in situ regolith on summits, sorted scree slopes and less regular talus slopes. Debris is then transported downslope by solifluction, which acts concurrently with frost sorting, responsible for the origin of patterned ground, particularly stone stripes. Slope-channel coupling, however, is limited. The diversity of periglacial landforms associated with frost-induced degradation of bedrock outcrops has developed in a relatively short time interval following deglaciation approximately 7,000 years, as suggested by dating from localities nearby.

Keywords: Periglacial, rock control in geomorphology, solifluction, hillslope sediment transfer, King George Island

Corresponding author: Piotr Migoń, piotr.migon@uwr.edu.pl

Introduction

Cold and wet environments of maritime Antarctica are characterized by a great diversity of periglacial processes and landforms, which are especially apparent on slopes and higher elevations rising several hundreds of metres above sea level (Lopez Martinez et al. 2012, Dąbski et al. 2017). In the relatively small areas of land freed from under the ice – often called ice-free oases – one can find diverse periglacial features, including patterned grounds such as stripes and sorted circles, solifluction landforms (solifluction lobes, tongues and sheets), talus slopes including protalus ramparts, rock glaciers, bedrock scars, and blockfields.

The ice-free oasis around the "Arctowski" Polish Antarctic Station belongs to the largest non-glaciated areas on King George Island, which is one among many islands forming the South Shetlands archipelago. Most of this currently ice-free area is distinguished by bedrock-controlled periglacial features that have formed since it was deglaciated. The efficacy of periglacial morphogenetic systems appears relief-dependent, reflecting significant altitude and

https://doi.org/10.14746/quageo-2024-0031
ISSN 2082-2103, eISSN 2081-6383

steepness variability within the oasis. Thus, steep slopes are shaped by rockfalls and, where scree exists, by mass movements such as debris flows. In contrast, in more inland, lower-relief settings geomorphic systems apparently operate at slower rates and show a rich inventory of landforms resulting from mechanical weathering and gravity-driven downslope movement of debris, mainly by solifluction. Periglacial landforms in the oasis were previously studied by Dutkiewicz (1982), as well as addressed in a comprehensive geomorphological assessment of the area by Kostrzewski et al. (2002). They were also considered in an attempt to look at the contemporary geomorphic system of the area from the perspective of a paraglacial sediment cascade (Zwoliński 2007, 2016). Nevertheless, the understanding of cold-climate morphogenetic systems of the oasis, especially of controls exerted by bedrock lithology and structure, is still incomplete. Little is known about the regional distribution and thermal properties of permafrost in this region, restricting our ability to assess the relative importance of various geomorphic factors in shaping ice-free terrain.

Among the secondary relief features within the plateau part of the study area is a small, but distinctive group of bedrock elevations, known as the Jersak Hills, underlain by columnar andesite. Field reconnaissance revealed considerable geomorphic diversity within this group, hypothesized to reflect structural complexity of andesitic lava flows. Consequently, the main aim of this research note is to document the geomorphic system of the Jersak Hills, emphasizing its relation to underlying geological structure and rock properties; hence, examining cold-climate landforms from a rock-control perspective. This approach appears effectively novel, despite numerous recent studies presenting periglacial morphogenesis in the unglaciated parts of the South Shetlands (Dutkiewicz 1982, Kostrzewski et al. 2002, López-Martínez et al. 2012, Dąbski et al. 2017, Oliva and Ruiz-Fernández 2017). The Jersak Hills are particularly suited to this kind of research, showing well-developed thermal jointing due to cooling of andesitic lava on one hand (Birkenmajer 1980, 1997b, Smellie et al. 2021), and – being a local elevation surrounded by flat-floored valleys – representing a complete weathering-hillslope geomorphic system on the other one. Thus, the study site may serve as a useful reference area for studies undertaken elsewhere, where bedrock properties are important controls of periglacial morphogenesis.

Geomorphic and geological setting

The wider study area (Fig. 1) encompasses c. 5 km^2. Except flat nearshore depositional areas in the east, occupied by marshes with relict beach ridges (Kostrzewski et al. 2002), the relief is hilly to mountainous, and predominantly denudational. Even though the maximum altitude is modest (320 m a.s.l.), relief along the coast in the northwestern part of the study area, overlooking the Ezcurra Inlet, is sufficient to have produced precipitous rock slopes and cliffs more than 100 m high, rock glaciers, and debris-mantled slopes as steep as 45°. Above these steep slopes the terrain is generally sloping gently in the opposite direction, to the southeast. Within this upland terrain local flats occur at various altitudes, up to 220 m a.s.l., which contain scattered low bedrock outcrops, separated by long low-angle slopes. Birkenmajer (1980) interpreted these flats as raised shore platforms with relict stacks and skerries. Nevertheless, unequivocal ancient beach deposits cannot be identified on these flats. To be sure, the flats have rounded clasts atop them, but these could have been produced by weathering alone or inherited from the pyroclastic deposits exposed in the study area. Valleys within the upland are generally wide and flat-floored, and they contain braided channels fed by melting snow patches. Only locally bedrock steps occur. The upland area was under ice until approximately 7000 years ago, as suggested by dates obtained in the adjacent Fildes Peninsula (Oliva et al. 2023), and subsequent deglaciation exposed bedrock surfaces (Birkenmajer 1997a). However, evidence for significant glacial imprint is rather scarce, whether erosional or depositional. In particular, evident roches moutonnées are absent within the upland surfaces. Instead, periglacial features are widespread and include patterned ground, sorted stripes, talus derived from frost shattering of bedrock, and ubiquitous gelifluction landforms (Dutkiewicz 1982).

Local bedrock is mainly volcanic and volcaniclastic rocks of basaltic and andesitic composition (Birkenmajer 1980, Smellie et al. 2021). The

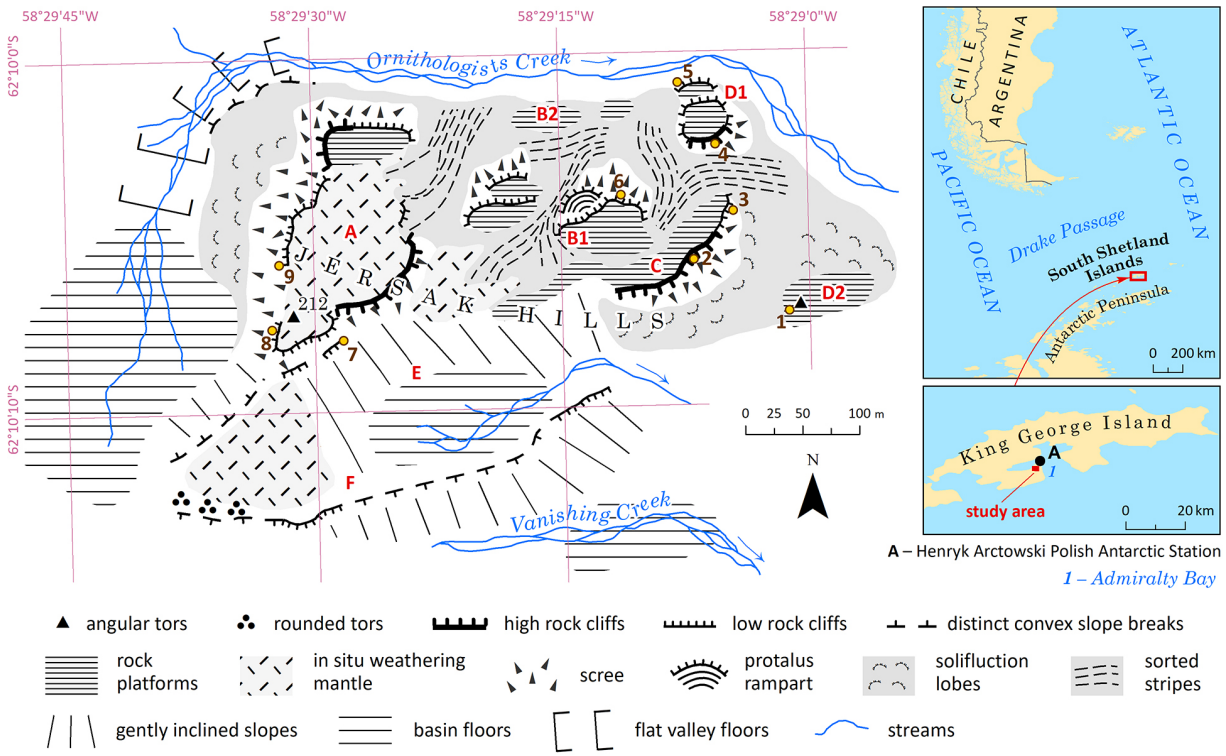

Fig. 1. Geomorphological sketch of the Jersak Hills and the position of study area in King George Island (map courtesy of Kacper Jancewicz). Letter codes A to F indicate distinctive parts of the study area and are referred to in text. Yellow circles and numbers 1 to 9 indicate localities where rock strength tests using Schmidt hammer were performed

outcrops of volcanic rocks analyzed in this paper are part of the Hennequin Formation, which consists of massive andesite lava flows alternating with breccia and tuff layers in the lower part, and lahar agglomerates with thin lava flows in the upper part. The formation is dated for the Eocene (Smellie et al. 2021) and is cross-cut by younger shallow intrusions which are either plugs, sills or dykes. Jardine Peak (280 m) dominating over the study area is a large plug modelled into a steep-sided cone, whereas the Jersak Hills – the subject of this study – were interpreted by Birkenmajer (1980) as a group of plugs and dykes. According to a more recent interpretation by Smellie et al. (2021), however, the outcrops expose lavas, with distinctive entablature jointing, although the thickness and geometric arrangement of columns are variable.

Methods

This study is primarily based on field mapping of periglacial landforms and evaluation of the factors that controlled their development. Although an ortophoto map at the scale 1:10,000 is available for the entire deglaciated oasis (Pudełko 2007), the resolution of the image proved insufficient to map specific landforms and field work became essential. Particular attention was paid to characteristic cold-climate landforms such as rock cliffs, scree slopes, solifluction lobes, snow-patch hollows, protalus ramparts, stone stripes, sorting features, and similar features characteristic of cold climates. The small size of the study area (less than 1 km^2) and easy access permitted ground checking of all critical locations. Heights of outcrops and horizontal distances were measured using TruPulse 3 laser rangefinder.

Schmidt hammer tests were performed at nine localities to determine intact strength of exposed andesite (Fig. 1). This was done in order to assess whether andesite may be differentiated into varieties of different strength, which might correlate with observed morphological differences (e.g., with slope steepness or outcrop height). An N-type Schmidt hammer was used and readings were collected perpendicularly to the rock face. Following the recommendations of Selby (1980) and Niedzielski et al. (2009), 25 readings

were taken at each site, with the results subject to standard statistical evaluation (the highest and the lowest values were discarded) and presented as box-plots. In addition, they were subject to testing for statistically significant differences between the sites using the Kruskal-Wallis test. To identify pairs of sites that differ significantly Dunn's multiple comparisons test was performed with the Benjamini-Yekuteili correction.

Field observations

Major landforms

The Jersak Hills comprise a roughly rectangular bedrock elevation, approximately 600 m × 450 m in plan, with the highest spot peaking at 212 m a.s.l. (Pudełko 2002). Relative relief in respect to the surrounding plateau is up to 60 m

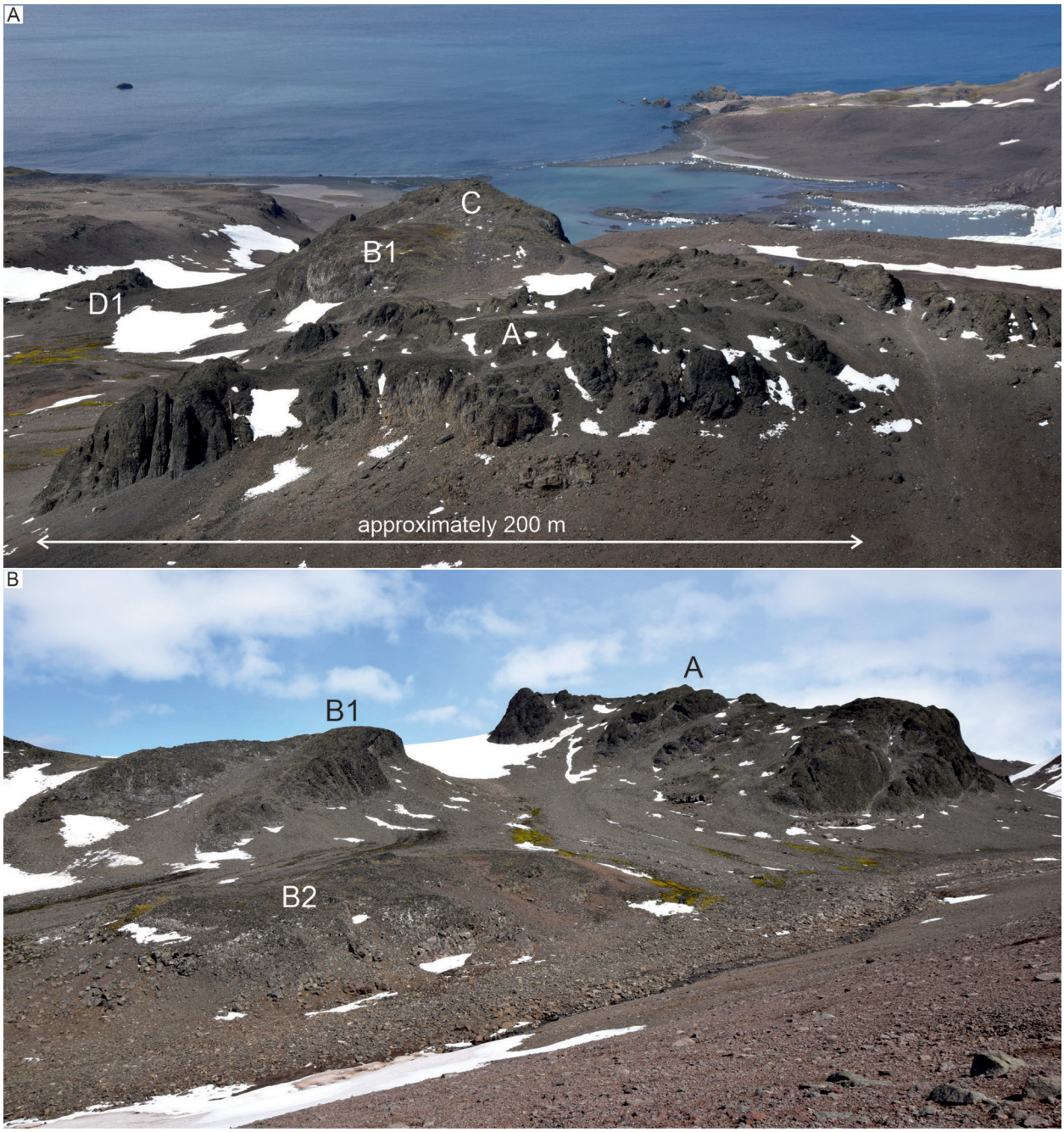

Fig. 2. Panoramic views of the Jersak Hills. A – from north-west, with the Admiralty Bay in the background; B – from north-east, with the valley of Ornithologists Creek in the foreground. Letters A to D1 indicate different parts of the study area, labelled on Fig. 1.

(Figs 1, 2). The shallow valley of Ornithologists Creek bounds the study area to the north and west, whereas the southern slopes terminate against the flat-floored valley of Vanishing Creek. The Jersak Hills consist of a few separate parts (Figs 1, 2). The largest bedrock outcrop is located in the west (A – see Fig. 1), rising steeply above the headwaters of Ornithologists Creek. A shallow N–S-trending trough separates this outcrop from two parallel lines of outcrops that trend W–E. Outcrops B1 (Fig. 1) are located at higher elevation and show morphological asymmetry. They consist of rock platforms grading into debris-covered surfaces in the south, but on the northern side they terminate as low rock cliffs. The B2 line includes platforms, but hardly any cliffs. An asymmetric arcuate ridge, with a precipitous slope facing south and east, and moderately sloping rock platforms atop, dominates the eastern part of the group (C – see Fig. 1), whereas two minor bedrock outliers occur in the north-east and extreme east (D1, D2 – see Fig. 1), the former with distinctive cliffs almost all around the perimeter. The surfaces between bedrock outcrops are regolith-covered, whereas elongated topographic lows sloping to the north act as transport corridors for rock debris produced by weathering. The southern part of the Jersak Hills is made of a wide regolith-mantled bench, locally waterlogged (E – see Fig. 1), which terminates against a low rocky scarp trending roughly WSW–ENE (F – see Fig. 1).

Jointing patterns, rock strength, and their impact on slope morphology

Each large bedrock outcrop mapped (Fig. 1) has its own specific shape and characteristic arrangement of columnar jointing. Two outcrops, the low ridge grading into a scarp in the south and labelled as F (Fig. 1), and the ridge C, are of considerable lateral extension and limited width, 400 m/15 m and 250 m/50 m, respectively. Other bedrock elevations are roughly equant and have vertical or steeply dipping columns, forming well-developed palisades, whereas some outcrops have columns arranged from horizontal to moderately dipping, up to 40° (Figs 1, 3). These structural differences control surface morphology of the outcrops.

Vertical columns are evident within the largest elevation A. Thin columns, approximately 10 cm wide on average, support rock cliffs which are up to 12 m high on the western side (Fig. 3A). In addition to regularly spaced thermal jointing, more prominent vertical fractures exist. Weathering has proceeded preferentially along these vertical fractures, thereby forming recesses in the rock face (Fig. 3A, E). The appearance of the upper surfaces of outcrops depends on the presence or absence of horizontal discontinuities. Outcrops D1 and D2 (Fig. 1) provide two contrasting examples of upper-surface morphology. The D2 outcrop is a low crag, 2 m in height. Densely spaced columns, only 5 to 10 cm apart, stand perfectly upright, accounting for the vertical sides of the outcrop and its jagged outline atop. However, despite similar vertical arrangement of columns within the D1 outcrop, the upper surface is nearly planar, probably following one of the sub-horizontal discontinuities. The spacing of vertical jointing is effectively uniform across most of the Jersak Hills, 10 cm on average. Larger spacing, 15–20 cm, is associated with higher cliffs, up to 14 m. In other places columns dip steeply, either into the slope (Fig. 3B) or the dip is approximately concordant with the slope. In the latter case, disintegration and separation of individual columns or their fragments is followed by downslope sliding (Fig. 3C). In some places, vertical and inclined columns grade into each other (Fig. 3D).

By contrast, entablature jointing exposed in the face of the outcrop C (Fig. 1) has an inverted fan-shape arrangement, lying flat in the central part (Fig. 3E) and rising towards both ends, to the inclination of 50 to 60°. The central part coincides with the highest rock cliff, 26 m in height. The flat-lying and dipping joints are crossed by vertical discontinuities that exhibit possible hydrothermal alteration in the form of clay infillings, exploited by weathering and debris removal to form rock wall recesses and steeply sloping ravines (Fig. 3F). In the eastern part of the outcrop these ravines cross-cut the dipping thermal joints, influencing the pattern of rock breakdown in the following way. The toppling of columns is associated within the slopes on the southern side, discordant to the dip, whereas sliding typifies dip-concordant slopes of the northern side. Both breakdown patterns may involve singular columns or thicker packets of several columns not separated from one another (Fig. 3D, lower right).

The outcrop F (Fig. 1) in the southern part of the area is incompletely exposed, as scattered, low bedrock knobs only 1–3 m high. Columnar jointing is absent and bedrock outcrops are of two kinds. Dense, roughly orthogonal pattern of joints supports low bedrock steps up to 2 m in height, whereas irregular joint patterns are associated with rounded shapes of outcrops, distinctively different from angular cliffs (Fig. 4A). The rock preferentially breaks down into subrounded clasts up to 20 cm in length (Fig. 4B). These characteristics and their contrasts to other parts of the Jersak Hills suggest that the outcrop F is not part of the andesite body, but more likely a separate basaltic lava unit.

In Schmidt hammer tests (Figs 1, 5), the mean intact strength of andesite varied from 50.48 to 39.78 and did not differ considerably between almost all of the test sites. The single exception to this uniformity is site 6 at the B1 outcrop which

Fig. 3. Different arrangements of columnar jointing in andesites of the Jersak Hills. A – narrowly-spaced vertical joints, with additional master joints spaced 1–3 m apart (cliffs are 12 m high); B – inclined columns dipping into the slope; C – inclined columns concordant with the slope (Schmidt hammer for scale); D – transition from vertical (right) to inclined columns (left); E – flat-lying columns exposed in a high cliff; F – vertical zones of hydrothermal alteration (marked by arrows).

yielded the highest average and median values and was shown to be statistically different from most of the other sites. This site also exhibits the largest spacing of joints (15–20 cm) and here the results of individual impacts were most consistent and yielded the lowest standard deviation. Although the cliff at this site is fairly high (14 m), it is surpassed by the more than 20 m high cliffs at site 2, which yielded a modest mean value of 45.3. The lowest mean value, in turn, was obtained at site 9, on a low cliff (approximately 3 m) that lacks clear columnar jointing, even though a similar test site next it (no. 8) yielded the third highest mean value of 45.96. Therefore, we hypothesize that intact rock strength plays subordinate role in determining morphological differences between the andesitic outcrops of the Jersak Hills. Rather, it appears that the geometrical arrangement of joints plays the major role.

Periglacial landforms, structures and cover deposits

The most prominent periglacial landforms in the study area area are screes and talus slopes, solifluction sheets, and stone stripes (Fig. 1). Scree slopes invariably exist along rock cliffs, testifying to efficient mechanical breakdown of andesite, facilitated by the dense spacing of primary joints. The most impressive are scree slopes below the highest cliffs, present on the south-eastern side of outcrop C and in the northwestern corner of elevation A (Fig. 1). The former reach 28 m in height from the cliff base to the toe and are divided into a steeper upper segment (35°) and less steep lower segment (25°) (Fig. 6A). Within the latter, a similar scree slope segmentation is present, with the upper cone inclined by 30° and the lower segment by 15–17° (Fig. 6B). In both cases the lower

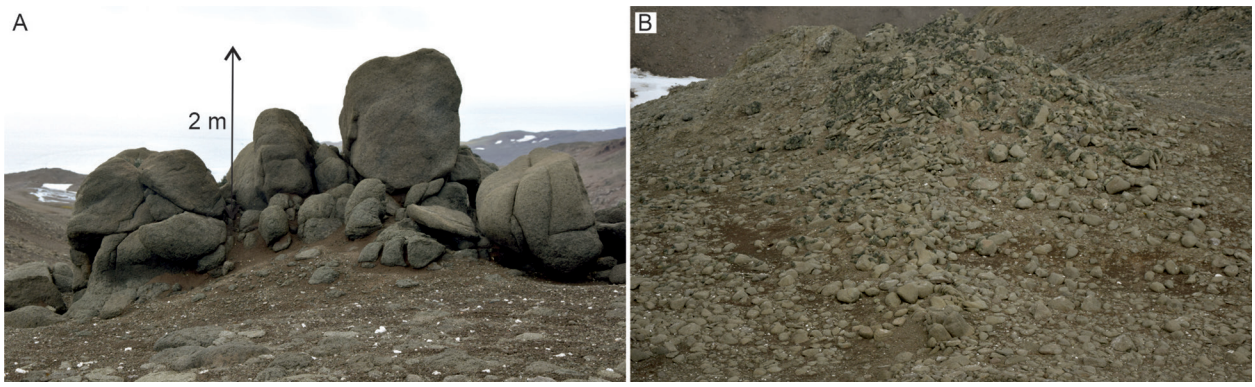

Fig. 4. Unlike andesites, typified by distinct columnar jointing, basalts are subject to spheroidal weathering and rounded boulders are produced. A – rounded low bedrock outcrop; B – abundant rounded boulders around an outcrop.

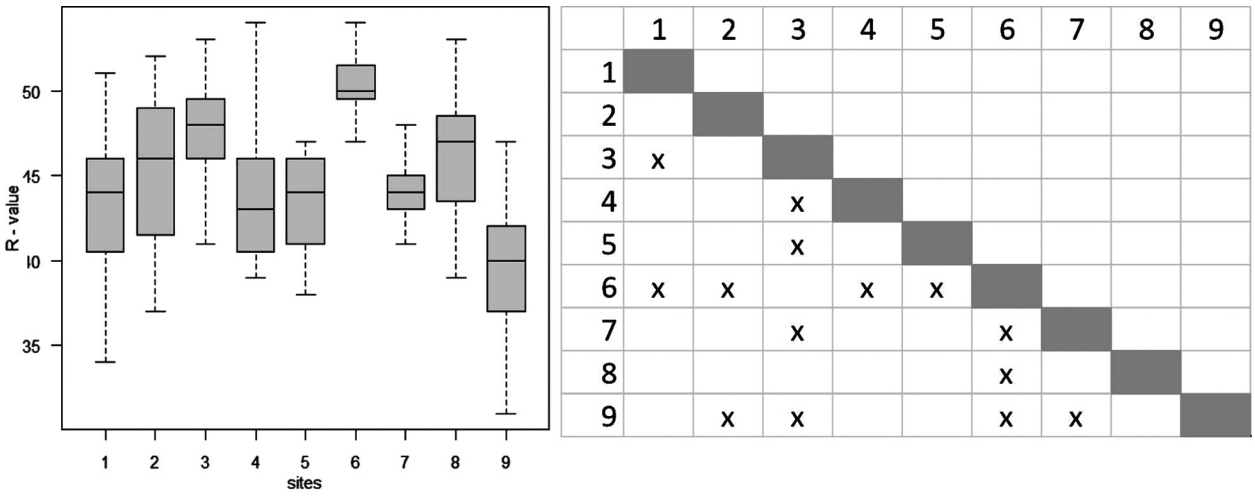

	1	2	3	4	5	6	7	8	9
1									
2									
3	x								
4			x						
5			x						
6	x	x		x	x				
7			x			x			
8						x			
9		x	x			x	x		

Fig. 5. Intact strength of andesites of the Jersak Hills measured by Schmidt hammer. Statistics of readings at each site on the left, results of statistically significant differences between the sites using Kruskal-Wallis test on the right.

segments terminate with distinct convex toes, 1 to 1.5 m high, slightly arcuate in plan view. Moreover, while the upper segments are built almost exclusively of angular debris, typically up to 10 cm in length, the lower segments are underlain by angular rock fragments mixed with finer, sandy-silty material. These lithological and morphological characteristics of the debris mantle are consistent with the gradual replacement of pure fall and slide from the rock cliffs by slow downslope movement of solifluction type. This slow movement is in turn retarded at the nearly flat footslope due to insufficient slope gradient so that the convex toes can form. Debris supply to the scree and talus slopes occurs mainly through the separation of segments of individual columns, but there is also evidence of occasional rock-slope collapses (falls or slides) involving larger volumes of material, including thick bundles of andesitic columns (Fig. 6C). Lower and inclined bedrock outcrops disintegrate mainly in situ and become partly buried under angular rock debris (Fig. 6D), which is difficult to erode away under such low-gradient conditions.

Solifluction mantles are widespread on slopes from as steep as approximately 25° to nearly planar footslope surfaces (Fig. 7A). The thickness of this mantle is unknown but the height of the convex toes suggests that it is at least 1 m. Locally, thickness may reach 3 m, on the basis of the heights of terminal scarps along Ornithologists Creek. Superimposed solifluction sheets and lobes are widespread, especially on the western side of rock outcrop A and the south-eastern side of rock outcrop C (Fig. 1). The near-surface parts of the solifluction mantle have been re-modelled by frost sorting, niveo-aeolian processes, and localized surface and shallow-subsurface wash, which all contribute to the emergence of downslope-elongated stone stripes. Runoff is responsible for the local erosion of fine material, resulting in open, grain-supported fabric of the

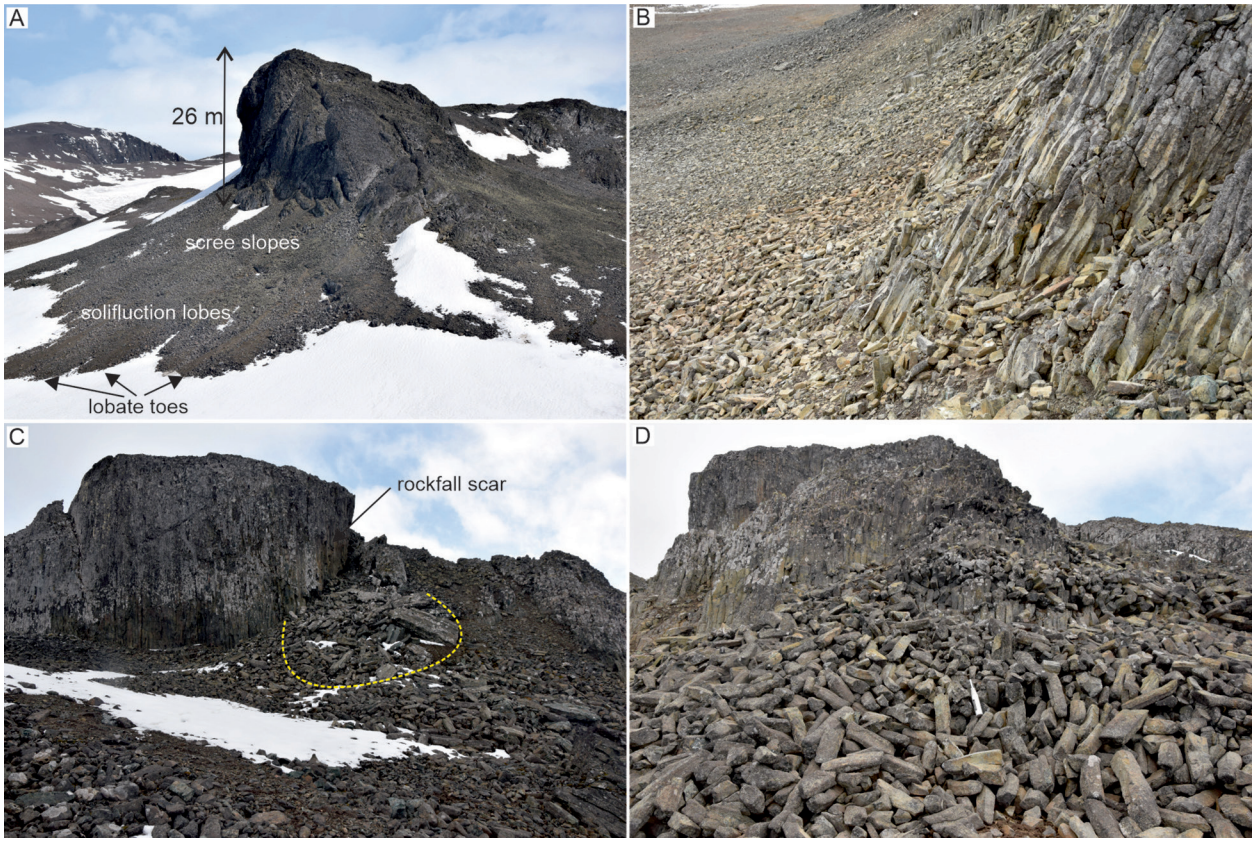

Fig. 6. Scree and talus slopes in the Jersak Hills. A – high scree slopes under rock cliffs more than 20 m high, with fall as the dominant supply. Lobate toes of solifluction lobes are highlighted by the upper limit of a snow patch; B – less inclined scree supplied mainly by sliding debris from inclined outcrops; C – debris pile from a rock-slope collapse (outlined by dashed yellow line); D – debris mantle derived from in situ rock disintegration (Schmidt hammer for scale).

debris mantle, which then consists only of larger clasts, 10 to 20 cm long (Fig. 7B). These stripes are 0.5 to 1 m in width, whereas the spacing between individual stripes is several metres. The irregular spatial pattern of bedrock highs and troughs sets the stage for different pathways of sediment transport. Thus, both convergent and divergent stone stripes have formed, depending on local slope configuration and slope angle (Fig. 7C,D). Thus, convergence occurs within the debris-filled troughs between outcrops A and B1. By contrast, diverging stone stripes have formed in the saddle between the outcrops B1, C and D2 (Fig. 1), being directed towards two topographic lows around the D1 crag (Fig. 1, 7D).

A distinctive landform exists at the foot of outcrop B1 (Fig. 1). It consists of an arcuate head scarp, a shallow hollow occupied by a snow patch, a moderately inclined (23°) debris slope, below the angle of repose, and an arcuate distal part terminated by a distinct toe 2 m high. The entire assemblage resembles a protalus rampart (see Shakesby 1997), although it is not backed by a high rock slope, but a low (10 m high), bedrock-controlled step. Nevertheless, the dense jointing of andesite exposed in the rock step facilitates efficient mechanical weathering, supplying rock debris to the slope below.

Slope-channel connectivity

Hillslopes in the study area are closely coupled to the local fluvial system, Ornithologists Creek (Figs 1, 2). Solifluction sheets and stone stripes are widespread along the northern slopes of the Jersak Hills, evincing movement of weathering-derived debris from the rock cliffs to the valley floor. However, the low gradient and low discharge of the creek reduce the possibility of effective further transport, although the distinct topographic step above the channel (Fig. 7B) suggests episodic undercutting of the toe of that slope and at least selective entrainment of slope debris by the stream. On the southern side, the

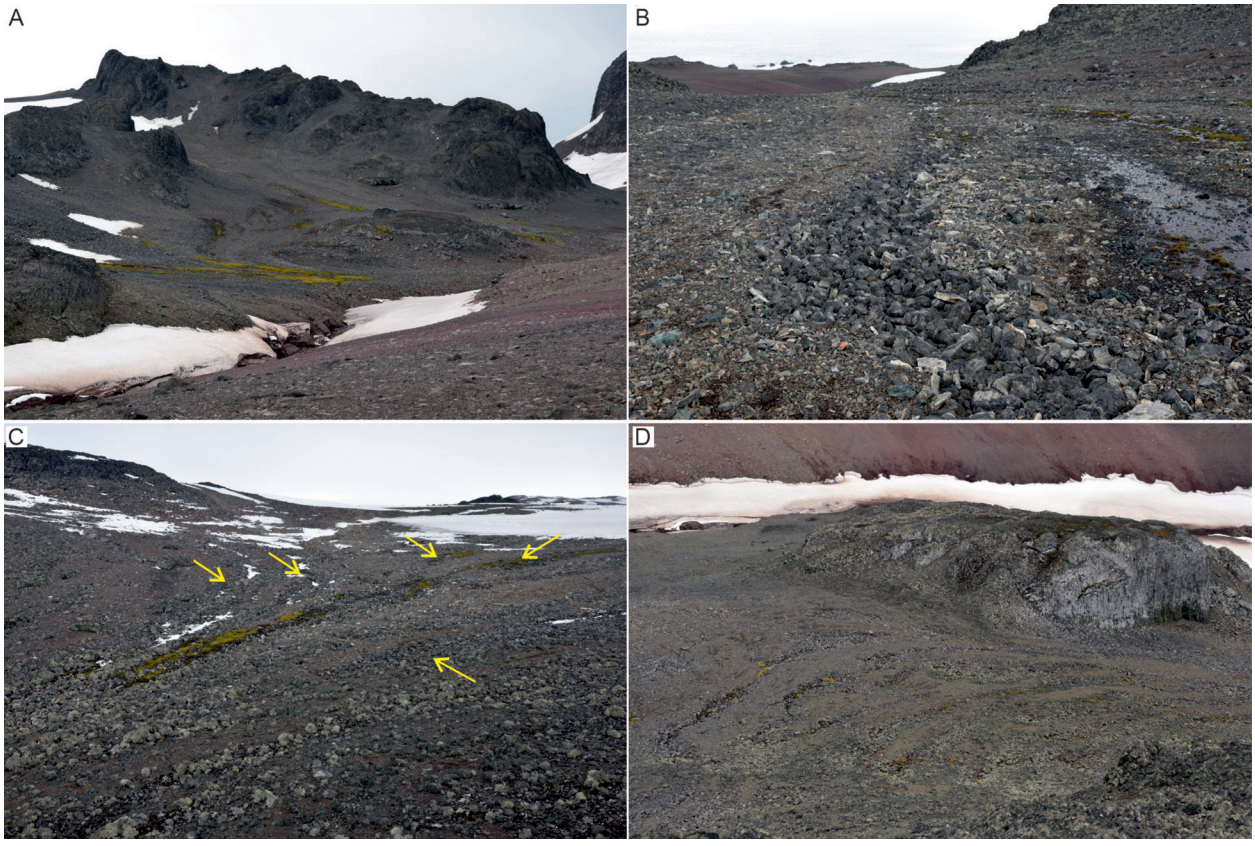

Fig. 7. Solifluction mantles and effects of combined frost sorting, surface and subsurface wash. A – general view of the hillslope sediment transfer system, from bedrock outcrops to the valley floor; B – open-work texture of a stone stripe (in the middle of the photograph); C – convergence of stripes (highlighted by arrows) in a topographic low; D – deflection of stripes to the right, around a bedrock outcrop located in the lower slope.

outcrop F (Fig. 1) provides a physical barrier between the upper and the lower slopes, so that gradual filling of the intermediate space (flat E, Fig. 1) may be inferred and no connection exists between the elevation of the Jersak Hills and the floor of the Vanishing Creek valley.

Hillslope periglacial system – a discussion

Despite its small size and relatively uniform geology (andesite and subordinate basalts), the periglacial geomorphic system of the Jersak Hills is diverse and includes various bedrock – landform – process connections. Even though the slopes are short, only attaining a maximum length of 250 m, typically less, their hillslope denudational systems integrate all essential elements. They include bedrock outcrops along local drainage divides, upper depositional slopes dominated by products of rock falls and topples, middle and lower depositional slopes shaped mainly by solifluction, footslopes receiving all debris from above, and valley/basin floors. Locally bedrock outcrops occur in the lower slopes too, complicating the system and influencing the pattern of debris movement.

Bedrock outcrops play a key role in the system, supplying debris and controlling system dynamics through their impacts on weathering and debris delivery. However, although the Jersak Hills are lithologically almost uniform, outcrops differ in terms of size, height, and morphology, especially columnar jointing. These differences impact the patterns and pathways of sediment transfer. Thus, the following settings may be distinguished: (1) high and typically vertical bedrock cliffs (>10 m), (2) low and more gently sloping bedrock cliffs (<10 m), and (3) rock platforms with occasional bedrock knobs. These three types of landforms are directly associated with debris-covered surfaces of different inclination. Consequently, the efficacy to transport weathering-derived material further away varies. High cliffs give way downslope to scree aprons (20–35°), whereas low cliffs coexist with less inclined depositional surfaces (10–20°). Rock platforms are even less inclined. The variety of bedrock outcrops in the study area seems to primarily reflect differences in structure, and the geometry of columnar jointing in particular, rather than variations in rock strength. This hypothesis could be tested by examining other ice-free areas on similar volcanic rocks. Generally, there is a close relationship between the orientation of rock columns and slope morphology, with vertical cliffs associated with either upright position of columnar jointing or their flat-lying geometry, whereas inclined columns produce sloping cliffs. However, they may also not give rise to cliffs at all, underlying moderately steep slopes covered by in situ debris instead.

Figure 8 illustrates the diversity of hillslope process-response systems in the study area. High cliffs are the most dynamic elements, subject to

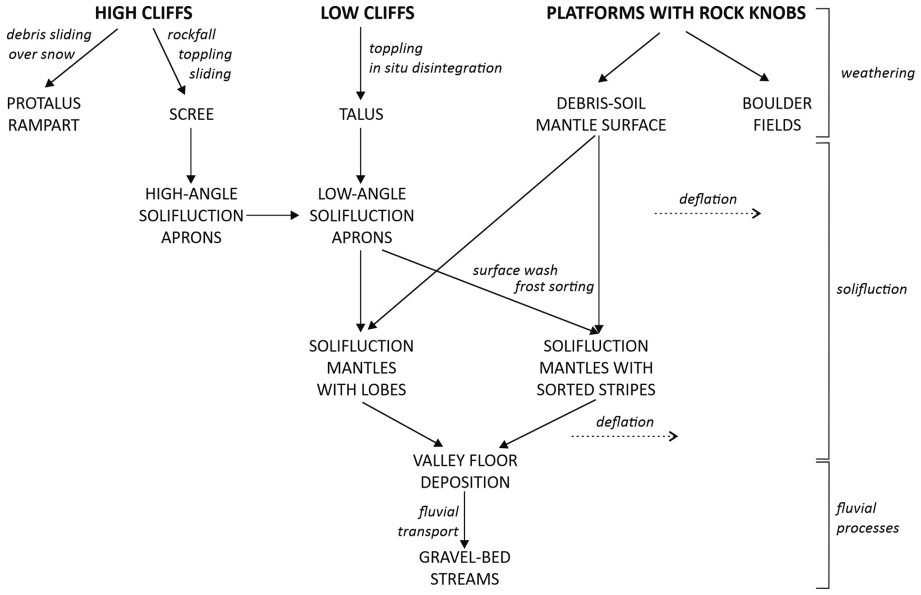

Fig. 8. Hillslope sediment transfer system of the Jersak Hills

rockfall and forward toppling that may involve individual columns or thick bundles of columns; in contrast, rock slides occur if columns are slightly inclined accordantly with the slope. These processes in combination produce scree resting at the angle of repose and, in some places, with superimposed larger rock fragments from more voluminous slope failures. Low and sloping cliffs are also subject to efficient mechanical disintegration, but the evacuation of debris is retarded due to comparatively low slope angle. Consequently, outcrops on these slopes tend to become buried in their own talus rather than are surrounded by scree. Outcrop F is a good example of a different style of degradation, caused by the massiveness of the rock and the absence of columnar jointing. Further weathering of angular debris within scree and talus supplies the finer sediment (sand, silt), required for solifluction to occur. Thus, scree slopes give way to high-angle (up to 25°) solifluction aprons, whereas talus landforms grade into low-angle aprons, with more evident lobate patterns than in their high-angle counterparts. These low-angle aprons may be also supplied by high-angle aprons directly underneath the high cliffs. Further downslope lobes become less distinct and the solifluction surfaces are of little relief. However, effects of frost sorting are evident locally and the study area presents striking examples of stone stripes, which are elongated parallel to the slope gradient. Bedrock control is evident here too, as topographic lows between bedrock outcrops channelize solifluction transport and the best developed stone stripes exist in these lows. Their open work structure suggests that, apart from solifluction, runoff from thawing snow patches is an important process (cf. Mitchell et al. 2023) and that deflation of fine material may occasionally take place under strong winds. Local flat-floored basins around the hills are long-term sediment traps for this fine sediment transported downslope. If there is a direct connection with the stream channel, the timeframe for storage at the slope to valley floor boundary may be of shorter duration and hillslopes effectively supply sediment directly to the fluvial system. However, this scenario only applies to the northern part of the study area (Fig. 1). Elsewhere, the hillslope system is not coupled with the fluvial one due to either too low gradient or the presence of bedrock barriers.

The extent to which glacial erosion processes may have preconditioned this periglacial system is unknown. No typical landforms of glacial erosion, such as polished surfaces and asymmetric roches moutonnées occur within the Jersak Hills. Moreover, rock cliffs face various directions and there is no preferential streamlining of bedrock outcrops. Nevertheless, the flattish summits of the contemporary bedrock outcrops, even though covered by angular products of andesite disintegration, may have roots in previous bedrock truncation by passing ice.

To be sure, some typical periglacial bedrock landforms are absent in the study area. No evidence of slope elements fitting the characteristics of cryoplanation terraces has been found and stepped slope profiles, with slope-perpendicular benches separated by risers, are absent (cf. Demek 1969, Thorn 2004). One explanation for the absence of these features is that terraces require protracted timescales to develop, perhaps tens to hundreds of thousands of years (Reger, Péwé 1976, Nyland, Nelson 2020, Mitchell et al. 2023), whereas the Jersak Hills were exposed only during the Holocene (Birkenmajer 1997b), and the present geomorphic system has not yet been in operation for sufficiently long. Nevertheless, geological structure may be a dominant control, such that the spatial patterns of resistant lava outcrops precludes the development of rock-cut landforms discordant to structure.

Conclusions

The study of periglacial landforms in the Jersak Hills documents the diversity of processes typical for wet and cold environments of maritime Antarctica and expands upon similar studies carried out in the vicinity (Dutkiewicz 1982, Kostrzewski et al. 2002, López-Martínez et al. 2012, Zwoliński 2016, Dąbski et al. 2017, Oliva and Ruiz-Fernández 2017), by including an assessment of bedrock properties. Freezing and thawing cycles affecting bedrock outcrops and regolith undoubtedly control the geomorphic system, in terms of both the origin of specific landforms and structures, as well as the efficacy of sediment transfer. However, the diversity and distribution pattern of landforms suggest that even under climatic conditions favouring

mechanical weathering the rock properties determine periglacial morphology. The study area has probably not been exposed long enough to permit the development of a bedrock-independent periglacial geomorphic system, with cryoplanation terraces as characteristic elements. Our study underscores the need for further research on the weathering efficiency in deglaciated ice-free areas of Antarctica, particularly considering the likelihood of rapid warming that may disturb the efficacy of typical cold-climate processes in bedrock-dominated terrains.

Acknowledgements

The authors are grateful to Kacper Jancewicz for drawing Figure 1 and to Milena Różycka for performing statistical tests. We also thank the reviewer, John Smellie, for correcting our presentation of geological background, and to R.M. Joeckel for thorough editing of the draft and useful suggestions for improvement.

Authors' contribution

P.M. – conceptualization; investigation; methodology; writing – original draft; writing – review and editing. M.S. – investigation; resources; writing – original draft.

References

Birkenmajer K., 1980. Geology of Admiralty Bay, King George Island (South Shetland Islands) – An outline. *Polish Polar Research* 1: 29–54.

Birkenmajer K., 1997a. Quaternary geology at Arctowski Station, King George Island, South Shetland Islands (West Antarctica). *Studia Geologica Polonica* 110: 91–104.

Birkenmajer K., 1997b. Thermal jointing in Tertiary volcanic plugs on King George Island, South Shetland Islands (West Antarctica) – a comparison with Tertiary volcanoes of Lower Silesia, Poland. *Studia Geologica Polonica* 110: 27–45.

Dąbski M., Zmarz A., Pabjanek P., Korczak-Abshire M., Karsznia I., Chwedorzewska K.J., 2017. UAV-based detection and spatial analyses of periglacial landforms on Demay Point (King George Island, South Shetland Islands, Antarctica). *Geomorphology* 290: 29–38. DOI 10.1016/j.geomorph.2017.03.033.

Demek J., 1969. Cryoplanation terraces, their geographical distribution, genesis and development. *Rozpravy ČSAV, ř. MPV* 79(4): 1–80.

Dutkiewicz L., 1982. Preliminary results of investigations on some periglacial phenomena on King George Island, South Shetlands. *Biuletyn Peryglacjalny* 29: 13–23.

Kostrzewski A., Rachlewicz G., Zwoliński Z., 2002. The relief of the western coast of Admiralty Bay, King George Island, South Shetlands. *Quaestiones Geographicae* 22: 43–58.

López-Martínez J., Serrano E., Schmid T., Mink S., Linés C., 2012. Periglacial processes and landforms in the South Shetland Islands (northern Antarctic Peninsula region). *Geomorphology* 155–156: 62–79. DOI 10.1016/j.geomorph.2011.12.018.

Mitchell R.J., Nelson F.E., Nyland K.E., 2023. Little tools, big job: The periglacial conveyor system in cryoplanated uplands. *Permafrost and Periglacial Processes* 34: 384–398. DOI 10.1002/ppp.2193.

Niedzielski T., Migoń P., Placek A., 2009. A minimum sample size required from Schmidt hammer measurements. *Earth Surface Processes and Landforms* 34: 1713–1725. DOI 10.1002/esp.1851.

Nyland K.E., Nelson F.E., 2020. Time-transgressive cryoplanation terrace development through nivation-driven scarp retreat. *Earth Surface Processes and Landforms* 45: 526–534. DOI 10.1002/esp.4751.

Oliva M., Ruiz-Fernández J., 2017. Geomorphological processes and frozen ground conditions in Elephant Point (Livingston Island, South Shetland Islands, Antarctica). *Geomorphology* 293: 368–379. DOI 10.1016/j.geomorph.2016.01.020.

Oliva M., Palacios D., Fernández-Fernández J.M., Fernandes M., Schimmelpfennig I., Vieira G., Antoniades D., Pérez-Alberti A., García-Oteyza J., ASTER Team, 2023. Holocene deglaciation of the northern Fildes Peninsula, KingGeorge Island, Antarctica. *Land Degradation and Development* 34: 3973–3990. DOI 10.1002/ldr.4730.

Pudełko R., 2002. *Ortophotomap Western Shore of Admiralty Bay, King George Island, South Shetland Islands*. Department of Antarctic Biology, Polish Academy of Sciences. IUNG, Puławy.

Pudełko R., 2007. *Site of Special Scientific Interest No. 8 (SSSI – 8). King George Island*. Department of Antarctic Biology, Polish Academy of Sciences. IUNG, Puławy.

Reger R.D., Péwé T.L., 1976. Cryoplanation terraces: indicators of a permafrost environment. *Quaternary Research* 6: 99–109. DOI 10.1016/0033-5894(76)90042-9.

Selby M.J., 1980. A rock-mass strength classification for geomorphic purposes: with tests from Antarctica and New Zealand. *Zeitschrift für Geomorphologie N.F.* 24: 31–51.

Shakesby R.A., 1997. Pronival (protalus) ramparts: a review of forms, processes, diagnostic criteria and palaeoenvironmental implications. *Progress in Physical Geography* 21: 394–418. DOI 10.1177/030913339702100304.

Smellie J.L., Hunt R.J., McIntosh W.C, Esser, R.P., 2021. Lithostratigraphy, age and distribution of Eocene volcanic sequences on eastern King George Island, South Shetland Islands, Antarctica. *Antarctic Science* 33: 373-401. DOI 10.1017/S0954102021000213.

Thorn C.E., 2004. Cryoplanation. In: Goudie A.S. (ed.), Encyclopedia of Geomorphology. Routledge, London: 204–205.

Zwoliński Z., 2007. Mobilność materii mineralnej na obszarach paraglacjalnych, Wyspa Króla Jerzego, Antarktyka Zachodnia. Wydawnictwo Naukowe UAM, Poznań.

Zwoliński Z., 2016. Solute and solid cascade system in the Antarctic oases. In: Beylich A.A., Dixon J.C, Zwoliński Z. (eds), Source-to-Sink Fluxes in Undisturbed Cold Environments. Cambridge University Press, Cambridge: 183–198. DOI 10.1017/CBO9781107705791.016.